

Article

Comparative Study of Tribological and Corrosion Characteristics of TiCN, TiCrCN, and TiZrCN Coatings

Aidar Kenzhegulov ^{1,*}, Axaule Mamaeva ¹, Aleksandr Panichkin ¹, Zhasulan Alibekov ¹, Balzhan Kshibekova ¹, Nauryzbek Bakhytuly ¹ and Wojciech Wieleba ²

¹ The Institute of Metallurgy and Ore Beneficiation, Satbayev University NJSC, Almaty 050013, Kazakhstan; a.mamayeva@satbayev.university (A.M.); a.panichkin@satbayev.university (A.P.); zh.alibekov@satbayev.university (Z.A.); b.kshibekova@satbayev.university (B.K.); n.bakhytuly@satbayev.university (N.B.)

² Faculty of Mechanical Engineering, Wrocław University of Science and Technology, 50-370 Wrocław, Poland; wojciech.wieleba@pwr.edu.pl

* Correspondence: a.kenzhegulov@satbayev.university; Tel.: +7-707-2000062

Abstract: Coatings based on titanium carbonitride alloyed with zirconium and chromium were deposited using the method of reactive magnetron sputtering on the surface of titanium VT1–0. The effect of alloying titanium carbonitride with zirconium and chromium on the tribo- and corrosion properties of the coating has been studied. Coatings with different compositions were formed by changing the ratio of alloying elements to titanium in a single target. To study the obtained coatings, a scanning electron microscopy, nanoindentation, sliding wear test (ball on disk method), and corrosion tests in 0.5 M Na₂SO₄ and 30% NaCl solution were used. As a result of wear and corrosion tests, friction coefficients, mass index, and corrosion rate of alloyed and pure titanium carbonitride coatings were obtained. The average coefficient of friction of the coatings varied in the range of 0.17–0.31. The values of nanohardness are determined depending on the composition of the coatings. From corrosion data, it is determined that TiCrCN and TiZrCN coatings exhibit better corrosion properties compared to TiCN coatings. As a result of the dependences obtained, the preferred composition of the coating, the most resistant to wear and corrosion damage, was revealed.

Keywords: titanium carbonitride; magnetron sputtering; alloying; friction coefficient; nanohardness; corrosion resistance; wear resistance



Citation: Kenzhegulov, A.; Mamaeva, A.; Panichkin, A.; Alibekov, Z.; Kshibekova, B.; Bakhytuly, N.; Wieleba, W. Comparative Study of Tribological and Corrosion Characteristics of TiCN, TiCrCN, and TiZrCN Coatings. *Coatings* **2022**, *12*, 564. <https://doi.org/10.3390/coatings12050564>

Academic Editor: Véronique Vitry

Received: 17 March 2022

Accepted: 14 April 2022

Published: 21 April 2022

Publisher's Note: MDPI stays neutral with regard to jurisdictional claims in published maps and institutional affiliations.



Copyright: © 2022 by the authors. Licensee MDPI, Basel, Switzerland. This article is an open access article distributed under the terms and conditions of the Creative Commons Attribution (CC BY) license (<https://creativecommons.org/licenses/by/4.0/>).

1. Introduction

Some machine components and structures are constantly subject to mechanical and chemical degradation due to wear and corrosion processes. Hard protective coatings greatly contribute to the wear and corrosion resistance of metals/metal alloys [1–5]. The use of hard protective coatings such as TiC [6], TiN [7], TiCN [8], TiAlN [9], TiSiC [10], Al₂O₃ [11], ZrTiCN [12], diamond-like films [13,14], and others is a suitable way to protect machine parts or tools from the harmful effects of the environment and wear. In these works, it is noted that coatings based on titanium carbides and nitrides provide good wear and corrosion resistance due to a combination of ductility and hardness, and high adhesion to the substrate.

To date, various physical and chemical deposition technologies have been used to obtain solid protective coatings. There are methods such as magnetron sputtering (MS) [15,16], cathode sputtering [17], plasma deposition [18], laser methods [19], methods based on chemical vapor deposition (CVD) [20], and others. Among them, MS is very often used for applying various hard tribological coating systems based on titanium carbonitride (TiCN) with increased wear resistance. MS provides a low level of impurities and allows easy control of the deposition rate. Depending on the deposition conditions, this method also makes it possible to obtain coatings with different morphology, structure, and properties.

TiCN-based coatings produced by this method exhibit a wide range of different properties such as high adhesion, wear resistance, and corrosion resistance.

One of the ways to improve the tribological and corrosion properties of TiCN coatings is alloying with various metals, such as O, Al, Ag, Si, Nb, Zr, Cr, etc. For example, the introduction of oxygen into the TiCN coating increases their resistance to friction and corrosion, which is justified by the inertness of the oxide and the small atomic size of oxygen, which creates high hardness and compressive stress [21,22]. Hsieh J.H. et al. [23] obtained a TiCNO coating and studied the effect of the oxygen content in the reaction atmosphere during magnetron sputtering on the properties of the TiCN coating. The results showed that the TiCNO coating obtained at an oxygen flow rate of 4 cm³/min has the lowest wear rate and highest nanohardness. Recently, in [24] the authors reported that the addition of Ag to the TiCN coating can improve friction and wear resistance at room and elevated temperatures. As a result of the work [25], the elemental ratio Ag/Ti (below 0.20) was determined, at which coatings with high mechanical properties are formed (hardness ~18 GPa, wear rate ~10⁻⁶ mm³/Nm). The purpose of the work [26] was aimed at studying the tribocorrosion behavior of TiSiCN nanocomposite coatings with a low coefficient of friction. The high wear resistance of the coating depended on the trimethylsilane flow rate. There are a sufficient number of works devoted to the above coatings in the literature. With regard to research on the effect of alloying with zirconium and chromium titanium carbonitride, their number is extremely limited.

Nevertheless, chromium alloying of TiCN coating is known [27]. The resulting films, which were prepared through co-sputtering of Ti, Cr, and graphite targets, exhibited high hardness (up to 40 GPa), low friction coefficient (0.03), and good wear resistance. The authors of [12] obtained (Zr,Ti)CN coatings for medical purposes by the MS method of two targets from Zr and Ti. The measured thickness and hardness of the coating were in the ranges of 1.8–2.1 μm and 25–29 GPa, respectively. Pruncu C.I. et al. [28] obtained TiCN coatings doped with Zr, Nb and Si. Zr, Nb and Si alloying elements in the film composition were in the range 2.9–9.6 at.% and ratio (C + N)/(sum of metals) was close to 1. In the result, the TiNbCN coating was found to have the best corrosion resistance due to the low residual stress and high adhesion to the substrate. From a comparative study [29] of (Zr,Ti)CN, (Zr,Hf)CN, and (Zr,Nb)CN coatings, it was found that films with higher non-metal content have finer morphology, higher hardness, and lower coefficient of friction. It is evident from the detailed work in this paragraph that the alloying process, which consists of adding chromium and zirconium to the main crystal structure of TiCN, is effective in improving the hardness and tribological properties of the coating. Despite these and other high-quality works, little information has been reported so far on the effect of Cr⁻ and Zr⁻ alloying on the properties of TiCN coatings deposited using a single target. Information on the analysis of the wear and corrosion characteristics of such coatings is very limited. In this regard, it seems interesting to study the effect of alloying with Cr and Zr on the corrosion and tribological characteristics of TiCN coatings. Thus, the aim of this study was to investigate the tribological and corrosion performance of TiCN, TiCrCN, and TiZrCN coatings using mechanical, tribological, and corrosion tests.

2. Materials and Methods

2.1. Substrate Preparation and Coating Process

TiCN, TiCrCN, and TiZrCN coatings were deposited in a 100 kHz pulsed direct current MS system. The distance between the target and the substrate holder was kept constant and amounted to 30 cm. To deposit pure TiCN, a target made of titanium VT1-0 (equivalent to titanium GRADE 2) was used, and composite targets were made to deposit TiZrCN and TiCrCN coatings (Figure 1). To do this, the alloying element in the form of a disk was welded onto the sputtered surface of the titanium target. Three and five disks of chromium and zirconium were welded onto the surface of the titanium target in order to change the composition of the obtained coatings. Well-polished plates (15 × 15 mm) and disks

(\varnothing 58 mm) made of titanium VT1–0 were used as substrates. The chemical composition of the substrate is shown in Table 1.



Figure 1. Titanium and composite targets after deposition of TiCN, TiCrCN, and TiZrCN coatings.

Table 1. Chemical composition of the titanium VT1–0 according to GOST 19807-91 [30].

Titanium Brand	The Content of Elements, No More, wt.%							
	Ti	Fe	Si	C	O	N	H	Other
VT1–0	99.24–99.7	up to 0.20	up to 0.1	up to 0.07	up to 0.2	up to 0.04	up to 0.01	up to 0.10

The schematic image of the preparation process of the titanium substrate and coating is presented in Figure 2. When preparing the surface of the substrates for sputtering, grinding was performed with P120 sandpaper, P180, P320, P600, P1000, P1200, P2000. Next, four-stage polishing with diamond paste was performed: 5/1 (3–5 μm), 2/1 (1–2 μm), 1/0 (1 μm), and final polishing on a clean wool cloth. After polishing, the substrates were washed with distilled water for 10 min and degreased with acetone. After performing the above processes, the substrates were placed in the working chamber. Before deposition, the chamber was evacuated to a base pressure below $3 \cdot 10^{-3}$ Pa. The MS facility is equipped with an APEL-IS-21CELL ion source (Applied Electronics, Tomsk, Russian Federation) and APELMRE100 magnetrons (Applied Electronics, Tomsk, Russian Federation). Before coating deposition, the substrates were ion cleaned with argon at an operating voltage of 2.5 kV, a current of 20–25 mA, and a pressure of 0.2 Pa for 20 min. The potential shift to the substrate was fixed at -70 V, which was supplied using an APEL-M-5PDC power supply (Applied Electronics, Tomsk, Russian Federation). This potential value was chosen on the basis of the results described in our previous work [31]. The flow rate of the inert and reactive gas was controlled using RRG–12 model flowmeters (Eltochpribor, Moscow, Russian Federation). Previously, composite targets were worked out in order to clean the surface from unwanted contaminants. The deposition parameters of all obtained coatings are presented in Table 2.

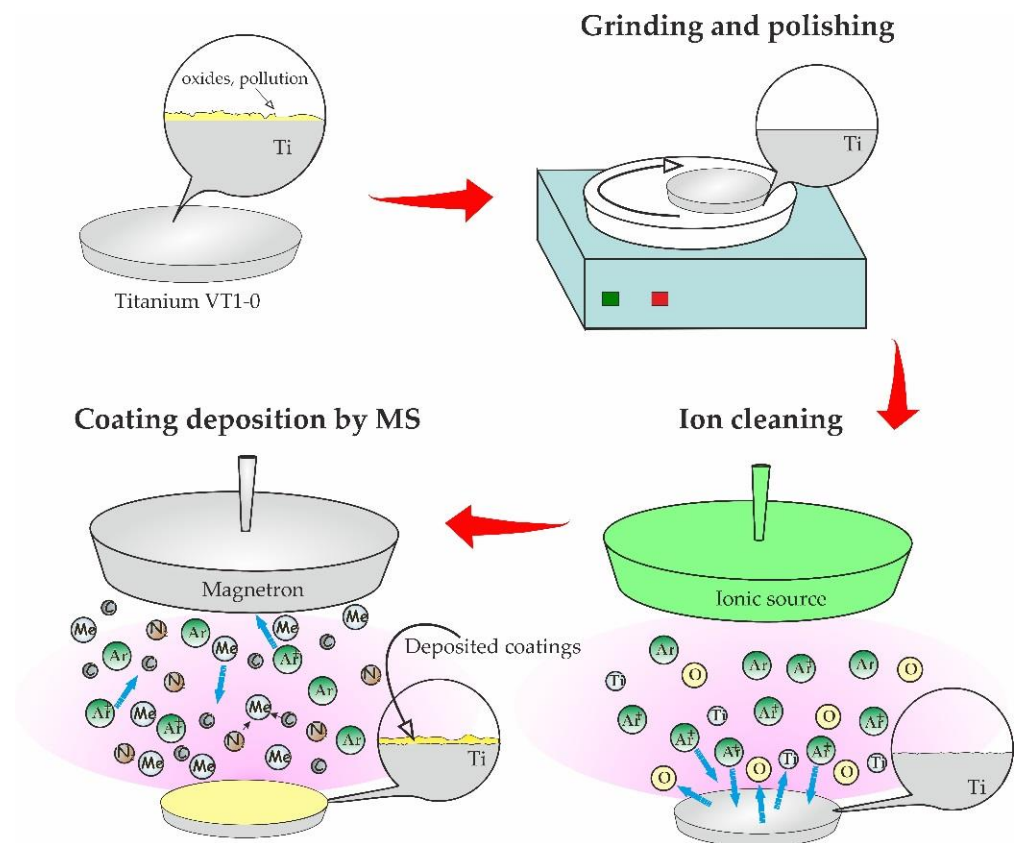


Figure 2. Scheme of the process of preparing the substrate and coating deposition.

Table 2. Magnetron sputtering parameters for the deposited coatings.

Coating	Coating Deposition Parameters				
	Target Type	Chamber Pressure, Pa	Flow of Inert and Reactive Gas, sccm	Plasma Current, A	Sputtering Time, min
TiCN	Ti	0.45	Ar = 18; C ₂ H ₂ = 3.6; N ₂ = 3	2	120
TiCrCN-1	Ti+Cr(3)	0.45	Ar = 18; C ₂ H ₂ = 4.6; N ₂ = 3	2	120
TiCrCN-2	Ti+Cr(5)	0.45	Ar = 18; C ₂ H ₂ = 4.6; N ₂ = 3	2	120
TiZrCN-1	Ti+Zr(3)	0.45	Ar = 18; C ₂ H ₂ = 4.6; N ₂ = 3	2	120
TiZrCN-2	Ti+Zr(5)	0.45	Ar = 18; C ₂ H ₂ = 4.6; N ₂ = 3	2	120

2.2. Morphology and Composition of Coatings

Surface morphology and coating thickness were studied by scanning electron microscopy (SEM). For these purposes, a JXA-8230 model electron microscope (JEOL, Tokyo, Japan) with an accelerating voltage of 25 kV and an electron beam current of up to 7 nA was used. All selected coatings were studied in the backscattered electron mode (Compo). To check the thickness of the coating, it was applied to glass. Then, using a glass cutter, a scratch was made on the opposite side of the glass substrate, and it was broken. As a result, the coating broke along with the glass. This made it possible to avoid blockages during sample preparation and more accurately determine the coating thickness using SEM. The elemental composition of the coating was analyzed using energy dispersive analysis of X-ray (EDAX) over the surface area of the coating $40 \times 40 \mu\text{m}^2$ at $\times 2000$ magnification.

The surface topography and roughness were studied by scanning probe microscopy (SPM) using a JSPM 5200 probe microscope (JEOL, Tokyo, Japan). The pictures were taken in semi-contact mode.

The phase composition and crystal structure of the coating were determined on a D8 Advance diffractometer (BRUKER, Karlsruhe, Germany) with α -Cu radiation ($\lambda \approx 1.54 \text{ \AA}$). Radiography was performed with focusing according to the Bragg–Brentano method. The diffraction patterns were recorded in the range of angles 2θ : $20\text{--}90^\circ$ with a step of 0.05° , a shooting rate of 2 deg/min at a voltage of 35 kV , and a current of 20 mA . The PDF 2 database was used for phase analysis.

2.3. Tribological Tests

To measure the tribological characteristics of the TiCN, TiCrCN, and TiZrCN coatings were deposited on the surface of a titanium VT1–0 substrate with a diameter of 58 mm . The tribological characteristics of the coatings were measured in the sliding friction mode according to the ball-on-disk scheme on a TRB³ tribometer (CSM Instruments, Peseux, Switzerland) at room temperature. The speed of movement of the sample surface relative to the counterbody is 1 cm/s , the load is 1 N , the radius of the wear track is 7 mm , the friction path is 100 m , the data acquisition rate is 50 Hz , and a ball of Si_3N_4 with a diameter of 6 mm was used as the counterbody. Test conditions are in accordance with international standards ASTM G99–959. The wear given in the work was calculated from the volumetric wear of the coatings during tribological tests. To do this, using a profilometer model 130, we measured the cross-sectional area of the wear track. Optical interference microscopy on a Leica DM IRM (Leica, Wetzlar, Germany) microscope was used to analyze the surface of the coating after testing the wear of the coating to describe the wear pattern.

2.4. Nanohardness

Nanoindentation was performed on a NanoScan–4D nanohardness tester (Nanoscan, Moscow, Russian Federation). Using a Berkovich indenter, 10 indentations were made at a load of 50 mN . The penetration depth of the indenter into the coating was $340\text{--}400 \text{ nm}$. Young's modulus and hardness were determined by the method of Oliver and Farr. Based on certain values, dependency graphs with a standard deviation were built.

2.5. Corrosion Testing

To measure the corrosion characteristics of TiCN, TiCrCN, and TiZrCN, coatings were deposited on the surface of VT1–0 titanium $15 \times 25 \times 1 \text{ mm}$ in size. The deposition was performed over the entire surface of flat substrates. Next, the coated plates were kept in a solution of $0.5 \text{ M Na}_2\text{SO}_4$ and $30\% \text{ NaCl}$ for corrosion testing. The exposure time was 720 h . After that, the corrosion characteristics were measured by the gravimetric method using an analytical balance of the brand Sartorius Cubis MSA3.6P (Sartorius, Goettingen, Germany) with an accuracy of $1 \text{ }\mu\text{g}$. Samples were weighed before and after soaking for 720 h in solutions. Using the weight data, the mass index and the corrosion rate were calculated. These data were obtained from the averages of the mass data of three coated plates.

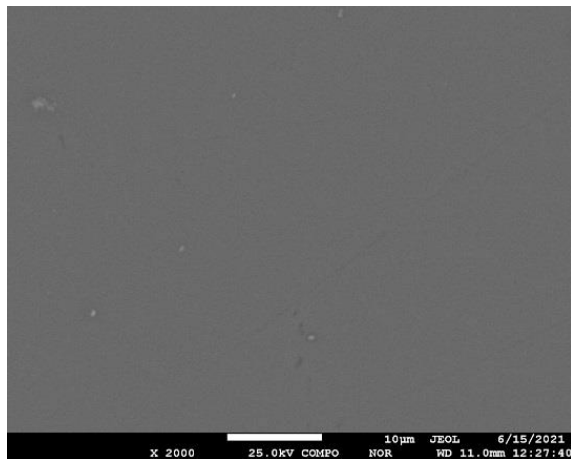
3. Results and Discussion

3.1. Morphology and Composition of Coatings

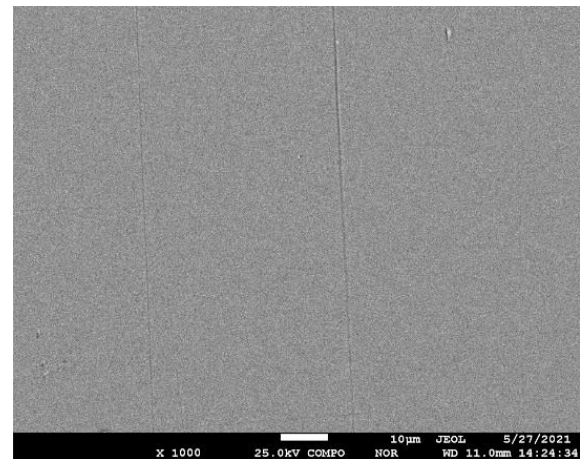
All obtained coatings characteristics are shown in Table 3. The surface morphology of the coating and the films thickness were measured using SEM. Figure 3 shows that the coating material was evenly distributed over the surface of the titanium substrate. The morphology of the coatings has a smooth and dense structure without visible defects. The image shows that on the surface of the samples there are sometimes dome-shaped nuclei. Significant changes in the surface morphology of the coating after alloying with zirconium and chromium are not observed. All coatings showed a similar surface structure. The measured coating thickness was approximately $1.4 \text{ }\mu\text{m}$ according to the SEM image.

Table 3. Value of the thickness, deposition rate, and roughness for the deposited coatings.

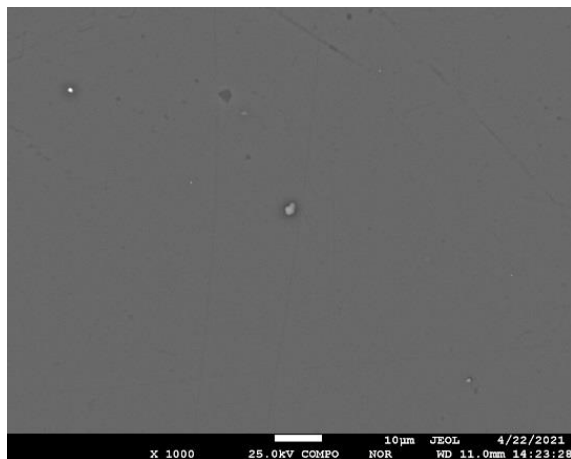
Coating	Coating Characteristics		
	Thickness, μm	Deposition Rate, nm/min	Roughness R_a , nm
TiCN	1.40	11.60	9.78
TiCrCN-1	1.55	12.91	4.30
TiCrCN-2	1.60	13.40	7.28
TiZrCN-1	1.74	14.50	2.50
TiZrCN-2	1.81	15.13	5.14



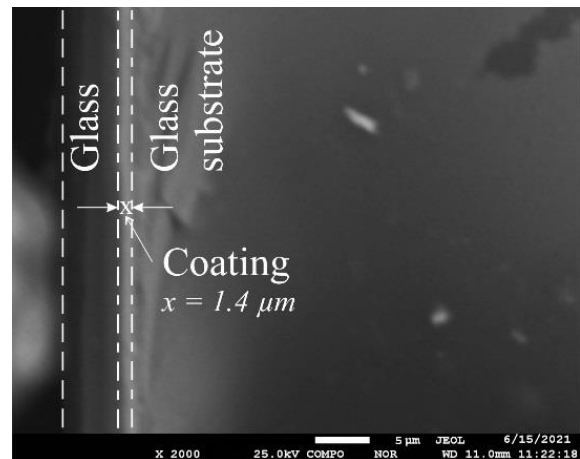
(a)



(b)



(c)



(d)

Figure 3. SEM images of the morphology of deposited coatings on titanium VT1-0 and the coating thickness on a glass substrate: (a) TiCN, (b) TiCrCN-1, (c) TiZrCN-1, and (d) thickness of TiCN coating.

Figure 4 shows two SPM images of the surface topography ($0.5 \times 0.5 \mu\text{m}^2$) of the TiCrCN-1 and TiZrCN-1 coatings. Similar results were obtained for other studied coatings. As can be seen from these figures, the surface of the coating has dense and smooth dome-shaped grains. Comparing the two coatings, it can be seen that TiZrCN-1 exhibits finer crystal grains. This may be due to an increase in carbon in the composition of this coating, as noted in the works [12,32].

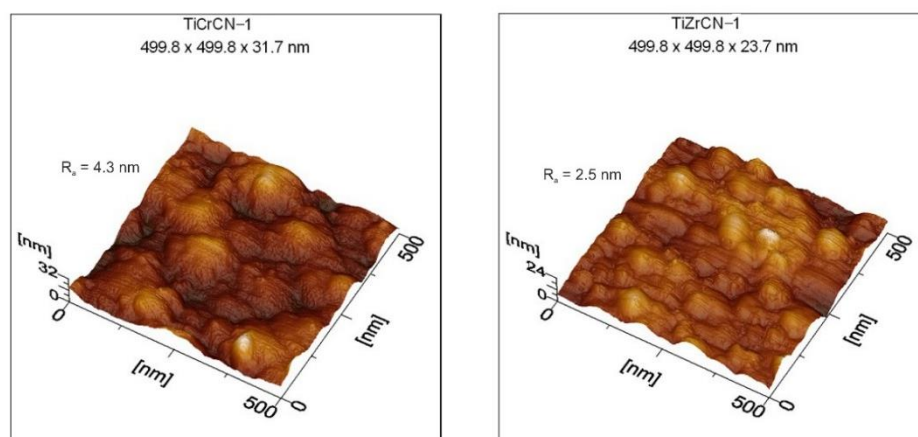


Figure 4. SPM images of the topography of deposited TiCrCN-1 and TiZrCN-1 coatings on titanium VT1-0.

Table 4 shows the composition of TiCN, TiCrCN, and TiZrCN coatings deposited at different ratios of alloying elements of the sputtered target. Coating composition was determined using EDAX. When alloyed with Cr and Zr, the composition of the coatings undergoes changes. Alloying leads to a decrease in the concentration of titanium and a variation in the concentration of carbon and nitrogen. The concentration of Cr and Zr in the deposited coatings increases with an increase in the number of disks of these metals on the surface of titanium targets. However, with an equal area of disks of alloying elements, the concentration of Zr in the deposited films is lower than the concentration of Cr. This is due to the difference in the sputtering coefficients of these metals. The stoichiometric composition according to the ratio $(C + N)/(\text{sum of metals})$ for TiCN was 0.87. When alloyed with chromium and zirconium, this ratio increased to 0.96 and 2.04, respectively. This behavior is clearly associated with a decrease in the metallic component. It is known that the ratio $(C + N)/(\text{sum of metals})$ should tend to 1, however, the results of some works show good results with a ratio greater than one: $(C + N)/(\text{Ti} + \text{Al})$ up to 1.75 [32], $(C + N)/(\text{Ti} + \text{Zr})$ up to 2.63 [12], and $(C + N)/(\text{Zr} + \text{Hf})$ [29] to 3.1.

Table 4. Elemental composition and $(C+N)/(\text{sum of metals})$ of deposited coatings.

Coating	Elemental Composition of Deposited Coatings, at. %					$(C + N)/(\text{Sum of Metals})$
	Ti	C	N	Cr	Zr	
TiCN	53.6	16.0	30.4	–	–	0.87
TiCrCN-1	34.1	28.7	19.7	17.5	–	0.94
TiCrCN-2	14.2	26.5	22.6	36.7	–	0.96
TiZrCN-1	20.8	34.7	32.4	–	12.1	2.04
TiZrCN-2	22.3	17.8	43.8	–	16.1	1.61

Figure 5 shows XRD patterns obtained for TiCN, TiCrCN-1, and TiZrCN-1 coatings. The diffraction patterns show that the following main phases were found in the coatings $\text{TiC}_{0.2}\text{N}_{0.8}$ and Ti_2CN for TiCN, $\text{Cr}_{0.2}\text{Ti}_{0.8}\text{C}$, $\text{TiC}_{0.25}\text{N}_{0.75}$, Ti_2CN for TiCrCN-1, and $\text{Ti}_{0.5}\text{Zr}_{0.5}\text{C}_{0.5}\text{N}_{0.5}$, TiZrC_2 for TiZrCN-1. The TiZrCN-1 coating shows a predominant orientation (111), which most likely indicates that in this layer the strain energy is dominant over the surface energy [33]. The diffraction peaks associated with TiZrCN-1 appear to be more intense compared to other coatings. TiCN and TiCrCN-1 coatings are characterized by the dominant crystallographic orientation (200). In TiCrCN-1 coatings, an amorphous halo is slightly noticeable. The amorphous phase is formed at large differences in atomic radii ($\text{Ti} = 0.147 \text{ nm}$, $\text{Cr} = 0.130 \text{ nm}$, $\text{Zr} = 0.160 \text{ nm}$), which creates a strong lattice distortion [34].

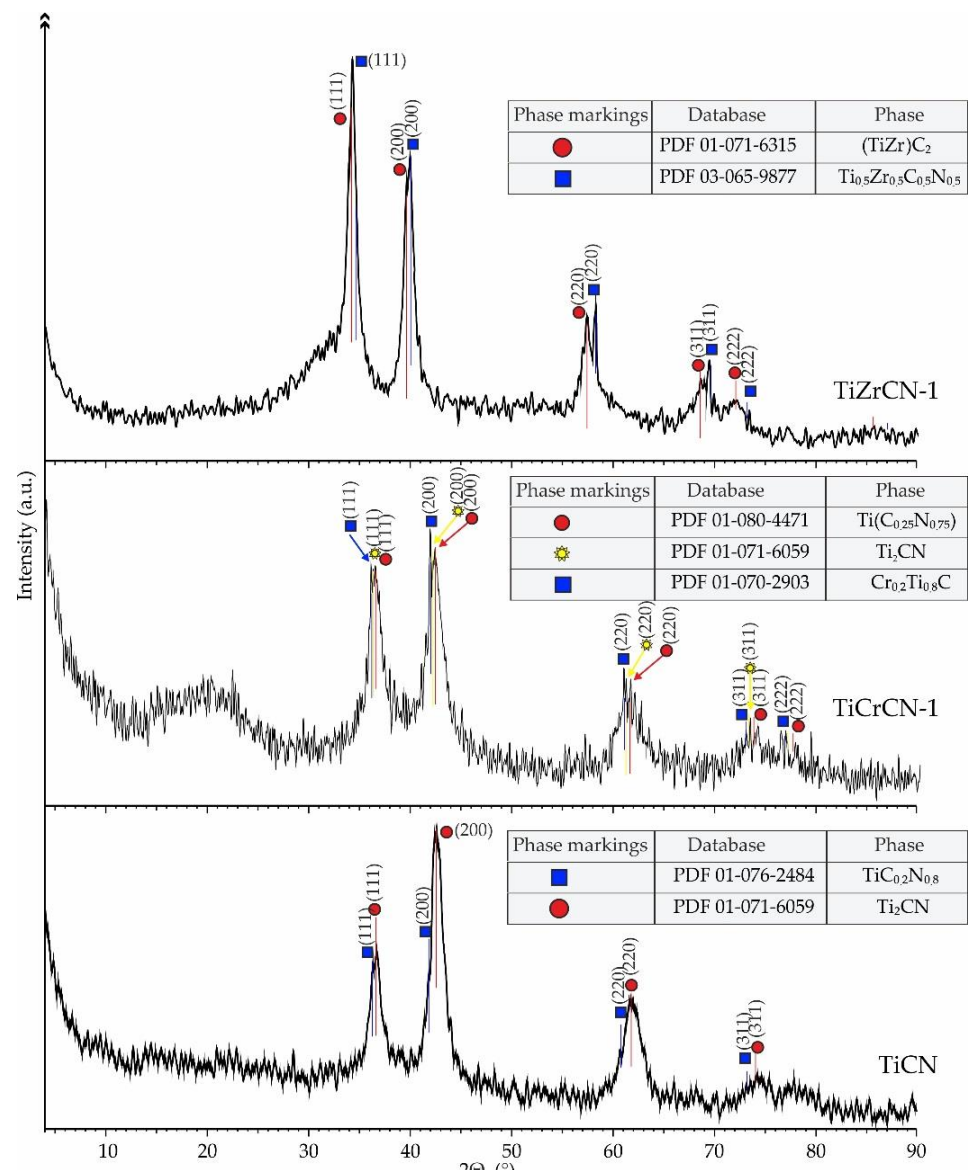


Figure 5. XRD patterns obtained for TiCN, TiCrCN-1, and TiZrCN-1 coatings.

3.2. Tribological Testing of Coatings

The wear resistance of TiCN coatings mainly depends on the microstructure, hardness, and adhesion, which are usually measured by determining the coefficient of friction and mass loss during wear [35]. The friction coefficient (CoF) of all coatings was measured relative to balls of Si₃N₄. The average CoF value was calculated after running a 100 m track. As a rule, the TiCN coating had a low CoF value. Figure 6 shows the graphs of CoF with the average value of all deposited coatings on titanium VT1-0. As can be seen from the results, TiZrCN coatings of 0.17–0.18 have the lowest CoF, while for TiZrCN-1 it is 0.17. In other cases, the CoF is close to 0.2, except for the TiCrCN-2 sample. This coating has a relatively high CoF with an average value of 0.31. The increase in CoF can be associated with a change in the composition at the friction interface between Si₃N₄ and the surface of the test sample. An increase in CoF after 20 m of track length for the TiCrCN-2 coating confirms the beginning of the coating degradation process, but without serious damage to the coating. The rest of the coatings show low CoF, which indicates a high cohesive and adhesive strength of the coatings formed by the MS method [36].

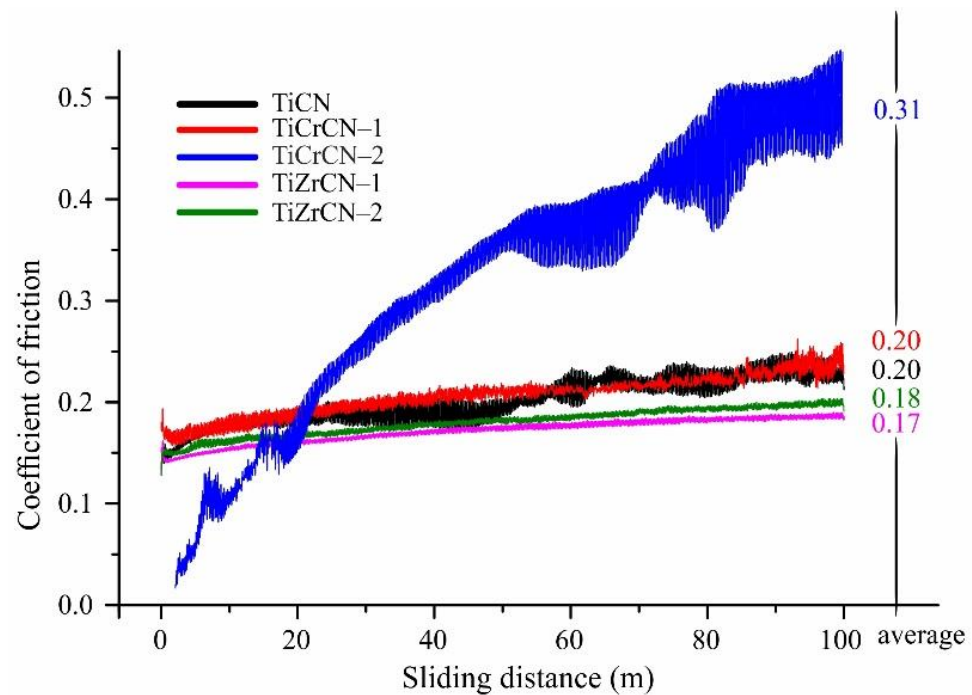


Figure 6. CoF with an average value for TiCN, TiCrCN, and TiZrCN coatings on a titanium VT1-0 substrate.

To compare the results, the wear test of the coatings was carried out under the same conditions in the ball-on-disk system using a Si_3N_4 counterbody (normal load 1 N, track length 100 m, track radius 7 mm). Table 5 and Figure 7 show these results. All coated specimens show wear tracks with varying groove widths that are parallel to the sliding direction. The presence of grooves parallel to the sliding direction indicates abrasive wear. On the surface of all coatings, debris, and in some places, uneven wear are observed in the place of friction. The TiZrCN coating is characterized by the highest wear resistance among the considered coatings, $3.35 \times 10^{-7} \text{ mm}^3/(\text{m}\cdot\text{N})$. Perhaps this is due to the low CoF and its high hardness. Comparison of wear track depth in SPM images of TiCrCN and TiZrCN coatings, then TiZrCN confirms the highest wear resistance of TiZrCN, since the wear track is hardly visible on its surface. It should be noted that the TiCrCN coating also has good wear resistance, the value of which is $8.4 \times 10^{-7} \text{ mm}^3/(\text{m}\cdot\text{N})$. As a result, it was found that coatings with high ratios $(\text{C} + \text{N})/(\text{sum of metals})$ can wear out slightly under friction conditions. In addition, these lower CoF and wear rates of the coatings can be explained by lower roughness (Table 3) [37], higher hardness [38], and H/E and H^3/E^2 values, which are presented in the next paragraph. In this way, alloying of Zr and Cr coatings from titanium carbonitride during their deposition on parts of machines and mechanisms can increase their service life, in comparison with parts coated with unalloyed TiCN films.

Table 5. The results of tribological investigations of TiCN, TiCrCN, and TiZrCN coatings.

Coating	Average CoF	Wear Track Width (mm)	Wear Loss Volume (mm^3)	Coating Wear Rate $\text{mm}^3/(\text{m}\cdot\text{N})$
TiCN	0.20	$0.21 \pm 0.16 \times 10^{-2}$	$4.81 \pm 2.33 \times 10^{-3}$	$1.9 \pm 0.58 \times 10^{-5}$
TiCrCN-1	0.20	$0.19 \pm 0.17 \times 10^{-2}$	$13.15 \pm 0.6 \times 10^{-5}$	$8.4 \pm 1.22 \times 10^{-7}$
TiCrCN-2	0.31	$0.45 \pm 0.2 \times 10^{-2}$	$2.48 \pm 1.1 \times 10^{-3}$	$4.14 \pm 1.83 \times 10^{-5}$
TiZrCN-1	0.17	$0.15 \pm 0.12 \times 10^{-2}$	$3.3 \pm 1.53 \times 10^{-5}$	$3.35 \pm 0.42 \times 10^{-7}$
TiZrCN-2	0.18	$0.33 \pm 0.02 \times 10^{-2}$	$11.3 \pm 2.3 \times 10^{-4}$	$5.4 \pm 3.9 \times 10^{-6}$

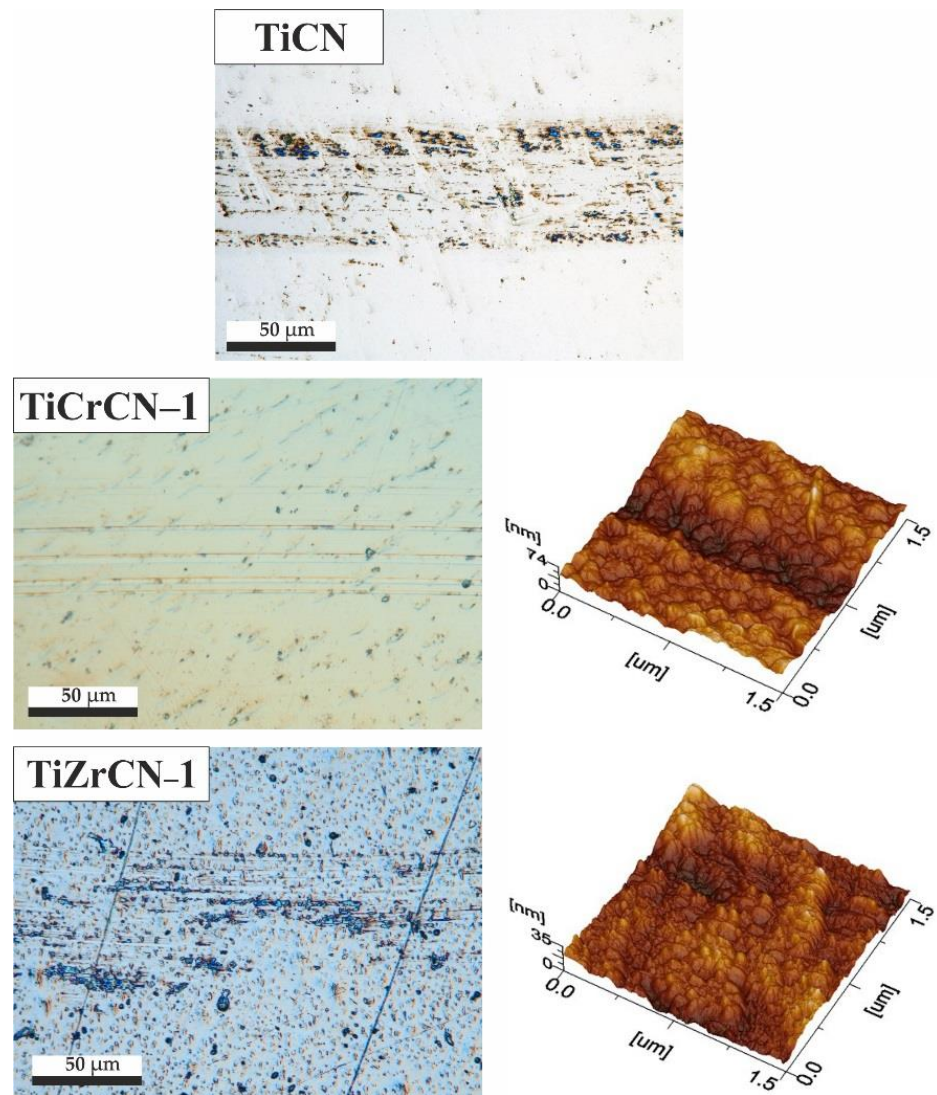
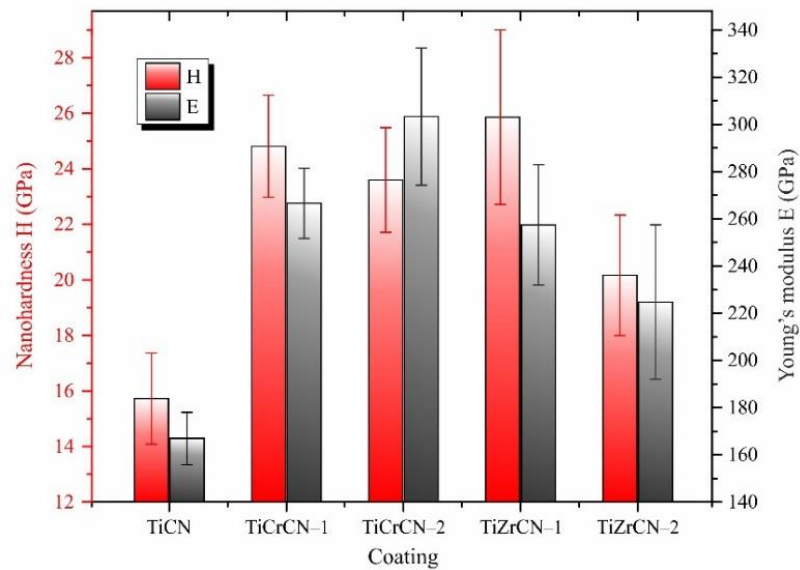


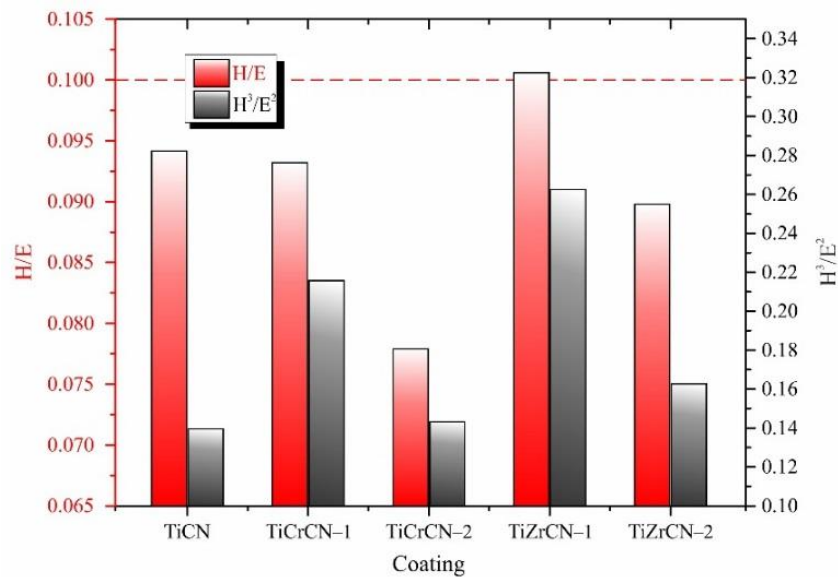
Figure 7. Optical micrograph and SPM images of the wear track of coatings after tribological tests.

3.3. Nanohardness of Coatings

Figure 8 graphically displays the values of nanohardness (H) and Young's modulus (E), calculated indicators H/E and H^3/E^2 for all obtained coatings, measured using nanoindentation. As can be seen from Figure 8a, alloying of the coating with Cr and Zr titanium carbonitride leads to an increase in nanohardness. High values are demonstrated by TiCrCN-1 and TiZrCN-1 coating, which have $H = 25$ GPa and $H = 26$ GPa, respectively. The Young's modulus of these coatings showed a high value around $E = 250$ – 260 GPa. This may be due to the low CoF and coating composition. The increase in nanohardness may be due to several factors, such as higher content of non-metals (Hall–Petch hardening effect) [39,40], grain reduction (Figure 4), solid solution hardening mechanism [41], and defect hardening mechanism [42], etc. Figure 8b shows the calculated ratios of nanohardness to Young's modulus, which can be considered as an indicator of good resistance to mechanical degradation and fracture [38]. Higher values ($H/E > 0.1$) may result in lower wear/loss rates [43]. From this point of view, the highest value of H/E and H^3/E^2 among the deposited coatings belongs to the TiZrCN-1 coating, which has $H/E > 0.1$, indicating good fracture resistance. The results of the H/E and H^3/E^2 values of this coating are correlated and confirmed by wear tests. It is interesting to note that the rest of the coatings have a lower H/E ratio than TiCN, but a higher H^3/E^2 ratio than TiCN.



(a)



(b)

Figure 8. Nanohardness data for TiCN, TiCrCN, TiZrCN coatings on titanium VT1–0: (a) nanohardness and Young's modulus, (b) H/E and H^3/E^2 values.

3.4. Corrosion Testing of Coatings

Corrosion performance is evaluated using corrosion rate and corrosion mass index. The mass corrosion index (K_m) shows how much the mass of the coating under study (Δm) has changed as a result of the corrosion process related to the unit of time (τ) and the metal surface area (S):

$$K_m = \Delta m / (S \times \tau) \quad (1)$$

Corrosion rate is the result of the effect of corrosion on a metal per unit of time. Using these two indicators of corrosion, dependency graphs were built. Corrosion tests were performed by immersing the obtained coatings into solutions of 0.5 M Na_2SO_4 and 30% NaCl.

Figure 9 shows the mass index and corrosion rate of all obtained coatings. The graph clearly shows that the corrosion resistance of TiCN coatings in both environments is well improved by alloying them with chromium and zirconium. In addition, in comparison, it is noticeable that the coatings show better resistance in a solution of 0.5 M Na₂SO₄ than 30% NaCl. According to the results of corrosion tests in the Na₂SO₄ solution, it was determined that the TiCrCN-2 coating has the lowest corrosion rate of 3.8×10^{-3} mm/year. This is most likely due to the high content of corrosion-resistant chromium (36.7 at.%). In contrast, the most rapidly corroding coating is TiCN, with a corrosion rate of almost 9×10^{-3} mm/year. A possible reason is that the TiCN film thickness is less than TiCrCN and TiZrCN. This means that the active substances can easily penetrate through the coating to the substrate.

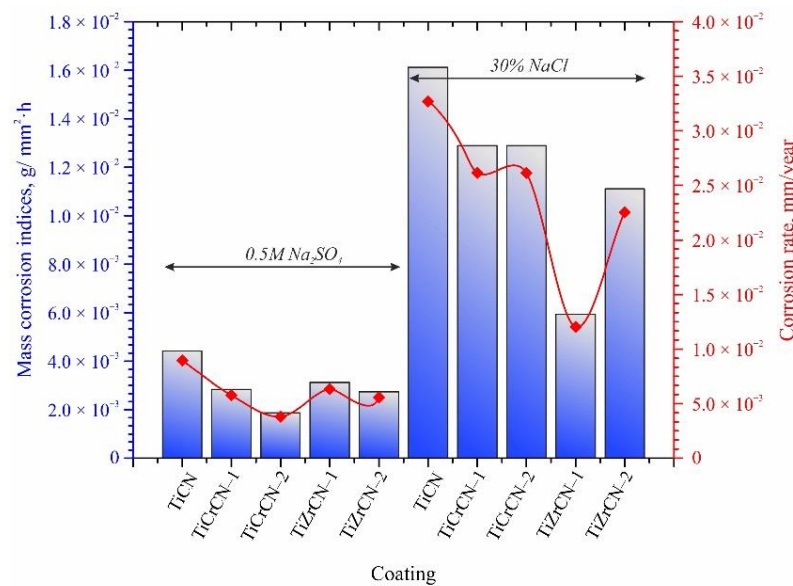


Figure 9. Corrosion indices of TiCN, TiCrCN, and TiZrCN coatings on a substrate of titanium VT1-0.

It follows from the results of corrosion tests in the NaCl solution that TiZrCN-1 has the lowest corrosion resistance at a rate of 1.2×10^{-2} mm/year. A possible reason for this phenomenon is that the carbon containing crystals in the structure of this coating can prevent the penetration of corrosive substances. Therefore, the NaCl solution had the least effect on this coating.

To summarize the results, it is clear from the corrosion data that the TiCrCN and TiZrCN coatings exhibit better corrosion properties than the TiCN coatings. This can be explained by the fact that alloying with TiCN promotes an increase in carbon and nitrogen in their crystal structure, which reduces the chemical activity [12,44].

4. Conclusions

TiCN, TiCrCN, and TiZrCN coatings were deposited by reactive magnetron sputtering at direct current on the surface of VT1-0 titanium in a reactive atmosphere of Ar, N₂, and C₂H₂. Five types of coating were deposited with different ratios (C + N)/(sum of metals) from 0.87 to 2.

The tribological and corrosion characteristics of the obtained coatings were studied. It has been determined that the friction coefficient decreases when alloyed with chromium and zirconium; in particular, TiZrCN coatings are characterized by the lowest friction coefficient with respect to the Si₃N₄ counterbody. Tribological testing showed high wear resistance of TiCrCN (up to 8.4×10^{-7} mm³/(m·N)) and TiZrCN (up to 3.35×10^{-7} mm³/(m·N)) coatings. Nanohardness analysis showed that alloying TiCN coatings with zirconium more significantly increases the hardness (26 GPa) compared to alloying with chromium (25 GPa). From the corrosion test results, it was revealed that the TiCrCN and TiZrCN coatings

demonstrate better corrosion properties compared to the TiCN coatings in 0.5 M Na₂SO₄ and 30% NaCl solutions.

In summary, the TiCrCN and TiZrCN coatings showed excellent performance in terms of tribological and corrosion resistance. Summing up the obtained comprehensive test results, we can single out the most preferable composition—the Ti₂₁Zr₁₂C₃₅N₃₂ (TiZrCN-1) coating, which is resistant to wear and corrosion damage. The resulting coatings can be useful as protection for machine parts or tools that are needed to counteract this.

Author Contributions: Conceptualization, A.M., A.P. and A.K.; methodology, A.K.; software, A.K. and N.B.; validation, A.M. and A.P. and W.W.; formal analysis, A.K. and B.K.; investigation, A.M. and A.K.; resources, A.K. and N.B.; data curation, A.M., A.K., A.P. and B.K.; writing—original draft preparation, A.K.; writing—review and editing, N.B. and Z.A.; supervision, A.M.; project administration, A.M.; funding acquisition, A.M. and A.P. All authors have read and agreed to the published version of the manuscript.

Funding: This research was funded by the Science Committee of the Ministry of Education and Science of the Republic of Kazakhstan, Grant No. AP08857049.

Institutional Review Board Statement: Not applicable.

Informed Consent Statement: Not applicable.

Data Availability Statement: The data and results presented in this study are available in the article.

Conflicts of Interest: The authors declare that there is no conflict of interest regarding the publication of this manuscript.

References

1. Srinath, M.K.; Ganesh, M.S.P. Wear and corrosion resistance of titanium carbo-nitride coated Al-7075 produced through PVD. *Bull. Mater. Sci.* **2020**, *43*, 108. [[CrossRef](#)]
2. Li, Z.; Di, S. The microstructure and wear resistance of microarc oxidation composite coatings containing nano-hexagonal boron nitride (HBN) particles. *J. Mater. Eng. Perform.* **2017**, *26*, 1551–1561. [[CrossRef](#)]
3. Ramazanova, J.M.; Zamalidinova, M.G. Physical and mechanical properties investigation of oxide coatings on titanium. *Complex Use Miner. Resour.* **2019**, *2*, 34–41. [[CrossRef](#)]
4. Almagul, U.; Bagdaulet, K.; Murat, O.; Azamat, Y.; Kaysar, K. Investigations of waste sludge of titanium production and its leaching by nitric acid. In Proceedings of the International Multidisciplinary Scientific Geoconference Surveying Geology and Mining Ecology Management SGEM, Albena, Bulgaria, 28 June 2019.
5. Yeshmanova, G.B.; Smagulov, D.U.; Blawert, C. Plasma electrolytic oxidation technology for producing protective coatings of aluminum alloys. *Complex Use Miner. Resour.* **2021**, *2*, 78–93. [[CrossRef](#)]
6. Kopf, A.; Haubner, R.; Lux, B. Double-layer coatings on WC-Co hardmetals containing diamond and titanium carbide/nitride. *Diam. Relat. Mater.* **2000**, *9*, 494–501. [[CrossRef](#)]
7. Matei, A.A.; Pencea, I.; Branzei, M.; Tranca, D.E.; Tepeş, G.; Tepeş, C.E.; Ciovica (Coman), E.; Gherghilescu, A.I.; Stanciu, G.A. Corrosion resistance appraisal of TiN, TiCN and TiAlN coatings deposited by CAE-PVD method on WC-Co cutting tools exposed to artificial sea water. *Appl. Surf. Sci.* **2015**, *358*, 572–578. [[CrossRef](#)]
8. Su, J.F.; Yu, D.; Nie, X.; Hu, H. Inclined impact-sliding wear tests of TiN/Al₂O₃/TiCN coatings on cemented carbide substrates. *Surf. Coat. Technol.* **2011**, *206*, 1998–2004. [[CrossRef](#)]
9. Gil, L.E.; Liscano, S.; Goudeau, P.; Le Bourhis, E.; Puchi-Cabrera, E.S.; Staia, M.H. Effect of TiAlN PVD coatings on corrosion performance of WC-6%Co. *Surf. Eng.* **2010**, *26*, 562–566. [[CrossRef](#)]
10. Rakhadilov, B.; Buitkenov, D.; Idrisheva, Z.; Zhamanbayeva, M.; Pazyzbek, S.; Baizhan, D. Effect of Pulsed-Plasma Treatment on the Structural-Phase Composition and Tribological Properties of Detonation Coatings Based on Ti-Si-C. *Coatings* **2021**, *11*, 795. [[CrossRef](#)]
11. Gassner, M.; Schalk, N.; Tkadletz, M.; Pohler, M.; Czettl, C.; Mitterer, C. Influence of cutting speed and workpiece material on the wear mechanisms of CVD TiCN/A-Al₂O₃ coated cutting inserts during turning. *Wear* **2018**, *398*, 90–98. [[CrossRef](#)]
12. Braic, V.; Braic, M.; Balaceanu, M.; Vladescu, A.; Zoita, C.N.; Titorencu, I.; Jing, V. (Zr,Ti)CN coatings as potential candidates for biomedical applications. *Surf. Coat. Technol.* **2011**, *206*, 604–609. [[CrossRef](#)]
13. Zhang, D.; Shen, B.; Sun, F. Study on tribological behavior and cutting performance of CVD diamond and DLC films on Co-cemented tungsten carbide substrates. *Appl. Surf. Sci.* **2010**, *256*, 2479–2489. [[CrossRef](#)]
14. Mansurov, B.; Medyanova, B.; Kenzhegulov, A.; Partizan, G.; Zhumadilov, B.; Mansurova, M.; Koztayeva, U.; Lesbayev, B. Investigation of microdiamonds obtained by the oxygen-acetylene torch method. *Eurasian Chem.-Technol. J.* **2017**, *19*, 163–167. [[CrossRef](#)]

15. Razmi, A.; Yesildal, R. Microstructure and mechanical properties of TiN/TiCN/TiC multilayer thin films deposited by magnetron sputtering. *Int. J. Innov. Res. Rev.* **2021**, *5*, 15–20. [[CrossRef](#)]
16. Chen, R.; Tu, J.P.; Liu, D.G.; Mai, Y.J.; Gu, C.D. Microstructure, mechanical and tribological properties of TiCN nanocomposite films deposited by DC magnetron sputtering. *Surf. Coat. Technol.* **2011**, *205*, 5228–5234. [[CrossRef](#)]
17. Matei, A.A.; Pencea, I.; Stanciu, S.G.; Hristu, R.; Antoniac, I.; Ciovica (Coman), E.; Sfat, C.E.; Stanciu, G.A. Structural characterization and adhesion appraisal of TiN and TiCN coatings deposited by CAE-PVD technique on a new carbide composite cutting tool. *J. Adhes. Sci. Technol.* **2015**, *29*, 2576–2589. [[CrossRef](#)]
18. Zhu, L.; He, J.; Yan, D.; Liao, H.; Zhang, N. Oxidation behavior of titanium carbonitride coating deposited by atmospheric plasma spray synthesis. *J. Therm. Spray Technol.* **2017**, *26*, 1701–1707. [[CrossRef](#)]
19. Yang, Y.; Guo, N.; Li, J. Synthesizing, microstructure and microhardness distribution of Ti–Si–C–N/TiCN composite coating on Ti–6Al–4V by laser cladding. *Surf. Coat. Technol.* **2013**, *219*, 1–7. [[CrossRef](#)]
20. Zhang, J.; Xue, Q.; Li, S. Microstructure and corrosion behavior of TiC/Ti(CN)/TiN multilayer CVD coatings on high strength steels. *Appl. Surf. Sci.* **2013**, *280*, 626–631. [[CrossRef](#)]
21. Stanishevsky, A.; Lappalainen, R. Tribological properties of composite Ti(N,O,C) coatings containing hard amorphous carbon layers. *Surf. Coat. Technol.* **2000**, *123*, 101–105. [[CrossRef](#)]
22. Olteanu, C.; Munteanu, D.; Ionescu, C.; Munteanu, A. Tribological characterisation of magnetron sputtered Ti(C, O, N) thin films. *Int. J. Mater. Prod. Technol.* **2010**, *39*, 186–194. [[CrossRef](#)]
23. Hsieh, J.H.; Wu, W.; Li, C.; Yu, C.H.; Tan, B.H. Deposition and characterization of Ti(C,N,O) coatings by unbalanced magnetron sputtering. *Surf. Coat. Technol.* **2003**, *163*, 233–237. [[CrossRef](#)]
24. Zhou, R.; Ju, H.; Liu, S.; Zhao, Z.; Xu, J.; Yu, L.; Qian, H.; Jia, S.; Song, R.; Shen, J. The influences of Ag content on the friction and wear properties of TiCN–Ag films. *Vacuum* **2022**, *196*, 110719. [[CrossRef](#)]
25. Sanchez-Lopez, J.C.; Abad, M.D.; Carvalho, I.; Escobar, G.R.; Benito, N.; Ribeiro, S.; Henriques, M.; Cavaleiro, A.; Carvalho, S. Influence of silver content on the tribomechanical behavior on Ag-TiCN bioactive coatings. *Surf. Coat. Technol.* **2012**, *206*, 2192–2198. [[CrossRef](#)]
26. Hatem, A.; Lin, J.; Wei, R.; Torres, R.D.; Laurindo, C.; Biscaia de Souza, G.; Soares, P. Tribocorrosion behavior of low friction TiSiCN nanocomposite coatings deposited on titanium alloy for biomedical applications. *Surf. Coat. Technol.* **2018**, *347*, 1–12. [[CrossRef](#)]
27. Zhang, S.; Fu, Y.; Du, H.; Zeng, X.T.; Liu, Y.C. Magnetron sputtering of nanocomposite (Ti,Cr)CNyDLC coatings. *Surf. Coat. Technol.* **2002**, *162*, 42–48. [[CrossRef](#)]
28. Pruncu, C.I.; Braic, M.; Dearn, K.D.; Farcau, C.; Watson, R.; Constantin, L.R.; Balaceanu, M.; Braic, V.; Vladescu, A. Corrosion and tribological performance of quasi-stoichiometric titanium containing carbo-nitride coatings. *Arab. J. Chem.* **2016**, *10*, 1015–1028. [[CrossRef](#)]
29. Braic, M.; Balaceanu, M.; Vladescu, A.; Zoita, C.N.; Braic, V. Study of (Zr,Ti)CN, (Zr,Hf)CN and (Zr,Nb)CN films prepared by reactive magnetron sputtering. *Thin Solid Films* **2011**, *519*, 4092–4096. [[CrossRef](#)]
30. GOST 19807-91 Wrought Titanium and Titanium Alloys. Grades GOST № 19807-91 from 17 July 1991. Available online: <http://vsegost.com/Catalog/28/28149.shtml> (accessed on 30 March 2022).
31. Mamaeva, A.; Kenzhegulov, A.; Panichkin, A.; Alibekov, Z.; Wieleba, W. Effect of Magnetron Sputtering Deposition Conditions on the Mechanical and Tribological Properties of Wear-Resistant Titanium Carbonitride Coatings. *Coatings* **2022**, *12*, 193. [[CrossRef](#)]
32. Stueber, M.; Barna, P.B.; Simmonds, M.C.; Albers, U.; Leiste, H.; Ziebert, C.; Holleck, H.; Kovács, A.; Hovsepian, P.; Gee, I. Constitution and microstructure of magnetron sputtered nanocomposite coatings in the system Ti–Al–N–C. *Thin Solid Films* **2005**, *493*, 104–112. [[CrossRef](#)]
33. Gall, D.; Kodambaka, S.; Wall, M.A.; Petrov, I.; Greene, J.E. Pathways of atomistic processes on TiN(001) and (111) surfaces during film growth: An ab initio study. *J. Appl. Phys.* **2003**, *93*, 9086–9094. [[CrossRef](#)]
34. Cahn, R.W.; Haasen, P. Physical metallurgy. *Phys. Metall.* **1996**, *1*, 1042–1048.
35. Mechri, H.; Saoula, N.; Madaoui, N. Friction and wear behaviors of TiCN coating treated by R.F magnetron sputtering. In Proceedings of the 7th African Conference on Non Destructive Testing ACNDT 2016 & the 5th International Conference on NDT and Materials Industry and Alloys (IC-WNDT-MI): Research Center in Industrial Technologies CRTI, Algiers, Algeria, 31 July 2016.
36. Kenzhegulov, A.K.; Mamayeva, A.A.; Panichkin, A.V. Adhesion properties of calcium phosphate coatings on titanium. *Complex Use Miner. Resour.* **2017**, *3*, 35–41.
37. Siow, P.C.; Ghani, J.A.; Ghazali, M.J.; Jaafar, T.R.; Selamat, M.A.; Haron, C.H.C. Characterization of TiCN and TiCN/ZrN coatings for cutting tool application. *Ceram. Int.* **2013**, *39*, 1293–1298. [[CrossRef](#)]
38. Musil, J.; Jirout, M. Toughness of hard nanostructured ceramic thin films. *Surf. Coat. Technol.* **2007**, *201*, 5148–5152. [[CrossRef](#)]
39. Hall, E.O. The Deformation and Ageing of Mild Steel: III Discussion of Results. *Proc. Phys. Soc. B* **1951**, *64*, 747–753. [[CrossRef](#)]
40. Petch, N.J. The Cleavage Strength of Polycrystals. *J. Iron Steel Inst.* **1953**, *174*, 25–28.
41. Holleck, H. Designing advanced coatings for wear protection. *Surf. Eng.* **1991**, *7*, 137–144. [[CrossRef](#)]
42. Jang, C.S.; Jeon, J.-H.; Song, P.K.; Kang, M.C.; Kim, K.H. Synthesis and mechanical properties of TiAlC_xN_{1-x} coatings deposited by arc ion plating. *Surf. Coat. Technol.* **2005**, *200*, 1501–1506. [[CrossRef](#)]

43. Leyland, A.; Matthews, A. On the significance of the H/E ratio in wear control: A nanocomposite coating approach to optimized tribological behavior. *Wear* **2000**, *246*, 1–11. [[CrossRef](#)]
44. Lou, J.; Gao, Z.; Zhang, J.; He, H.; Wang, X. Comparative investigation on corrosion resistance of stainless steels coated with titanium nitride, nitrogen titanium carbide and titanium-diamond-like carbon films. *Coatings* **2021**, *11*, 1543. [[CrossRef](#)]